International Journal of Computational and Experimental Science and ENgineering (IJCESEN)

Vol. 10-No.2 (2024) pp. 102-111
http://www.ijcesen.com

ISSN: 2149-9144

Research Article

A novel approach for Technetium-99m radioisotope transportation and storage in lead-free glass containers: A comprehensive assessment through Monte Carlo simulation technique

Duygu Sen BAYKAL*

Istanbul Nisantasi University, Faculty of Engineering and Architecture, Mechatronics Engineering, Istanbul, Türkiye
* **Corresponding Author Email:** duygu.senbaykal@nisantasi.edu.tr - **ORCID:** 0000-0001-9833-9392

Article Info:

DOI: 10.22399/ijcesen.304
Received : 21 March 2024
Accepted : 29 April 2024

Keywords

Lead-free Glass
Radioisotope Containers
Shielding Parameters
MCNPX
Phy-X/PSD

Abstract:

The primary aim of this project is to develop glass containers that are free from lead for the transportation of Tc-99m. The analysis included glass container structures characterized by the chemical formula $60B_2O_3$-(25-x)GeO_2-15BaO-xWO_3 (where x ranges from 0 to 25). The rates of addition, in theory, range from 3.397 to 4.124 g/cm^3. To evaluate the radiation shielding abilities of glass containers, the Phy-X/PSD software was used. The energy values employed in the evaluation varied from 0.015 MeV to 0.15 MeV, a range frequently employed in the field of medical physics. The transmission factors for the specific gamma energy of Tc-99m were determined using the Monte Carlo method MCNPX (version 2.7.0). This method enables the accurate simulation of particle motion and interaction. The G6 glass container type exhibited the highest level of gamma-ray attenuation among all the investigated glass containers, primarily due to its superior shielding properties. The creation of glass containers that do not contain lead and are designed to contain the movement of Tc-99m has significant implications in the areas of radiopharmaceuticals and medical diagnostics. In light of the continuous attempts of the scientific community, it is advisable to undertake more investigations aimed at enhancing the technology of lead-free glass.

1. Introduction

The process of ionization and the subsequent wave or particle transmission of energy over space or a material medium are both brought about by radiation, which is the energy that may free bound electrons from atoms. There are several places where radiation may be found; some are naturally occurring, like the sun and some earth minerals, while others are man-made, including X-ray machines and nuclear power plants. Radiation is useful in many different contexts, such as cancer treatment, medical imaging, and sterilization [1]. However, the ionizing property of radiation can result in both harmful consequences and benefits when used for diagnosis and treatment within specific dose limits [2-3]. Technetium-99m (Tc-99m), an artificial element with atomic number 43, is commonly used in medical physics, especially in nuclear medicine imaging techniques. Tc-99m, one of its most well-known isotopes, is often used in single-photon emission computed tomography (SPECT) scans because it has many useful properties, such as a short half-life and the right amount of energy for gamma-ray emission. Technetium-based radiopharmaceuticals are given to patients intravenously in medical imaging to accumulate specifically in target tissues or organs. Specialized imaging devices detect the emitted gamma rays to visualize and diagnose medical conditions such as cancer, heart disease, and bone disorders [4]. Tc-99m has multiple important qualities that make it ideal for medical imaging purposes. The half-life of around 6 hours balances decay rate and imaging duration, providing adequate imaging time without exposing patients to prolonged radiation. The gamma-ray energy of approximately 141 keV is ideal for penetrating biological tissues and being detectable by imaging devices, resulting in clear and precise images [5]. Shielding, involving the creation of barriers using dense materials, is one of the most effective methods to prevent radiation exposure. Lead has been widely used for radiation attenuation due to its high density and effectiveness. Its malleability allows it to be easily shaped into various shielding materials for different applications

in radiation-exposed areas [6]. Despite its effectiveness, the use of lead has raised significant health and environmental concerns over time. Problems with the nervous system, retardation in development, and damage to internal organs are among the long-term effects of lead exposure. In response to these concerns, there is an increasing trend towards lead-free options in industries where radiation shielding is crucial. Modern lead-free glasses are now recognized as a practical alternative for radiation shielding purposes. These glasses are made using alternative heavy metals and metal oxides like barium, bismuth, and tungsten, offering similar shielding properties to lead without the associated health risks. Lead-free glasses are also more environmentally friendly and easier to recycle compared to lead-containing glasses. Various factors need to be considered when creating lead-free glass for radiation shielding, including the type and energy of radiation, the required thickness and density of the glass, and properties like optical clarity [7-13]. The design of a glass storage container for technetium in medical diagnostics is a challenging task due to the necessity of safe and efficient transportation. The container needs to offer sufficient shielding to reduce radiation exposure to personnel and maintain the integrity and stability of the technetium radiopharmaceutical. An optimal glass storage container should be crafted with multiple essential features in mind. The material should be made of high-density glass that can effectively reduce gamma radiation. Tc-99m is essential for modern medical imaging, and creating a glass storage container for its transportation involves careful planning for radiation shielding, containment, and usability. By incorporating new materials and design principles, these containers can improve safety and efficiency in the handling and transportation of technetium radiopharmaceuticals, ultimately benefiting both patients and medical professionals [14-16]. Gamma energy is crucial for developing shielding materials compatible with technetium-based radiopharmaceuticals. This ensures the images are precise and safeguards individuals from radiation exposure. Therefore, the aim of this study is to enhance safety and efficiency in the field of medical imaging by developing lead-free glass storage containers for the safe and effective transportation of technetium radiopharmaceuticals.

2. Material and Methods

This study include $60B_2O_3$-(25-x)GeO_2-15BaO-xWO_3 (x=0, 5, 10, 15, 20, 25) composite glass sytem, which is include boric oxide, barium, germanium oxide, and tungsten trioxide, with these additive rates theoretical ρ range from 3.397 to 4.124 g/cm^3. Boric oxide demonstrates resistance to high levels of ionizing radiation. Boron enhances the absorption of radiation, making glass with boron a powerful shield against nuclear radiation. Germanium oxide can influence properties such as optical and mechanical characteristics. Barium is known for its effectiveness in blocking gamma rays. Barium oxide enhances the radiation attenuation properties of glass by facilitating radiation absorption. Tungsten trioxide enhances the radiation shielding capacity of glass due to its high resistance to gamma rays [17-19]. The chemical compositions of the investigated glass compositions are listed below, and the elemental weight fractions are shown in Table 1.

- $60B_2O_3$-$25GeO_2$-$15BaO$-$0WO_3$ (ρ=3.397 g/cm^3)
- $60B_2O_3$-$20GeO_2$-$15BaO$-$5WO_3$ (ρ=3.542 g/cm^3)
- $60B_2O_3$-$15GeO_2$-$15BaO$-$10WO_3$ (ρ=3.688 g/cm^3)
- $60B_2O_3$-$10GeO_2$-$15BaO$-$15WO_3$ (ρ=3.979 g/cm^3)
- $60B_2O_3$-$5GeO_2$-$15BaO$-$20WO_3$ (ρ=3.833 g/cm^3)
- $60B_2O_3$-$0GeO_2$-$15BaO$-$25WO_3$ (ρ=4.124 g/cm^3)

Table 1. *The glass container codes, elemental weight fractions, and densities of all investigated glass types.*

Codes	Elemental weight fraction (wt.%)					Density (g/cm^3)
	B	O	Ge	Ba	W	
G1	0.1863	0.5058	0.1735	0.1344	-	3.397
G2	0.1863	0.5008	0.1388	0.1344	0.0397	3.542
G3	0.1863	0.4959	0.1041	0.1344	0.0793	3.688
G4	0.1863	0.4910	0.0694	0.1344	0.1190	3.833
G5	0.1863	0.4860	0.0347	0.1344	0.1586	3.979
G6	0.1863	0.4811	-	0.1344	0.1982	4.124

2.1 Gamma-ray Shielding Parameters

2.1.1. Linear attenuation coefficient

A relationship can be expressed in the domain of radiation experimental research as follows:

$$I(x) = I_o e^{-\mu x} \quad (1)$$

where μ denotes the material's linear attenuation coefficient and compares the counts of attenuated and unattenuated gamma-rays I(x) passing through a thickness (x) material [20-22].

2.1.2. Mass attenuation coefficient

Mass attenuation coefficients are utilized to determine the linear attenuation coefficient ($\mu_m = \mu/\rho$) for different materials. Mass attenuation coefficient formulas are utilized in various fields, such as medical imaging. These coefficients are

essential for determining the radiation absorption rates of different materials [20-22].

2.1.3. Half-value layer

As it interacts with a target, the half-value layer (HVL) causes the radiation to be half as intense as it was before it passed through. You may figure out the half-value layer (HVL) by using this formula:

$$HVL = \frac{ln(2)}{\mu} \quad (2)$$

where μ represents the linear attenuation coefficient of the material. This measurement is essential for evaluating the efficacy of shielding materials in radiation protection [20-22].

2.1.4. Tenth-value layer

Measuring in centimeters and expressed as a percentage of the overall material thickness, the tenth value layer (TVL) is the thickness of the layer that is needed to decrease the main value of photon counts by one-tenth. The tenth value layer is commonly utilized to characterize the ability of X-rays or gamma rays to penetrate a particular material [20-22].

$$\text{TVL} = \frac{ln(10)}{\mu} \quad (3)$$

2.1.5. Mean free path

The formula for calculating the mean free path (mfp), another shielding parameter, is as follows: the distance a particle travels before potential collisions with other particles.

$$\text{mfp} = 1/\mu \quad (4)$$

where μ is the collision cross section of the material. This parameter helps determine the effectiveness of a material in stopping or slowing down particles passing through it [20-22].

2.1.6. Effective atomic number

The composite material's Compton scattering interaction process has an impact on a parameter known as the effective atomic number (Z_{eff}), which is [20-22];

$$Z_{eff} = \frac{\sigma_T}{\sigma_e} \quad (5)$$

2.1.7. Effective electron density

The effective electron density, or N_{eff}, is an additional important parameter that describes the radiation interaction of a material. The material's electron density is what determines the calculation [20-22].

The study evaluated all radiation shielding parameters using Phy-X/PSD software. The software enabled precise simulations of different shielding materials and thicknesses, offering valuable data for enhancing radiation protection strategies. This thorough analysis will help create and execute successful shielding strategies in different radiation settings [23].

2.2. MCNPX (Monte Carlo N-Particle eXtended)

The Monte Carlo method is an effective computational technique that approximates solutions to intricate mathematical and physical problems by utilizing random sampling. The method is based on generating random samples from probability distributions that are pertinent to the problem being addressed. The samples are utilized to model the behavior of a system or process, enabling the calculation of quantities like probabilities, expected values, or performance metrics [24-26]. The Monte Carlo approach follows the trajectories of particles entering a material medium based on the premise that their characteristics and interactions with matter follow certain statistical distributions. All probabilities are recorded for each monitored particle. When radiation beams interact with matter, changes in their energy and trajectories complicate the development of an analytical function to solve particle transport in any material medium. The Monte Carlo N-Particle Simulation Method (MCNP) algorithm is used to describe the radiation source, the materials it will interact with, and the detectors that will be used for computer-based measurements. The MCNP algorithm categorizes input data for simulating radiation transport issues in a computer environment into three basic groups: cell, surface, and detector definitions. The first stage in converting these notions to a computer system is to establish the concept of empty space. The second phase involves constructing an experimental setup inside the vacant area utilizing codes that include cell, surface, and detector definitions for data processing [27].

2.3. Designing Geometry in MCNPX

Its ability to manage stochastic processes, intricate geometries, and nonlinearities makes it a crucial tool for researchers and practitioners aiming to

comprehend and enhance systems in uncertain and random conditions. Geometry is crucial in the Monte Carlo method within computational modeling and simulation, influencing the precision, effectiveness, and relevance of simulations in different fields. The Monte Carlo method is known for its ability to effectively solve complex problems using random sampling, but it requires accurate representation of geometric structures and boundaries to produce valid results. The Monte Carlo method simulates system behavior by tracking particle trajectories and interactions within a defined geometric space [24-26]. This space includes the boundaries, materials, and structures that are pertinent to the issue under investigation. Precise geometry modeling is essential as it directly impacts the likelihood of particle interactions, scattering events, and the overall movement of energy and matter in the system. Accurate geometric representations are crucial for modeling the absorption and deflection of radiation in different materials and obstacles in radiation transport and shielding.

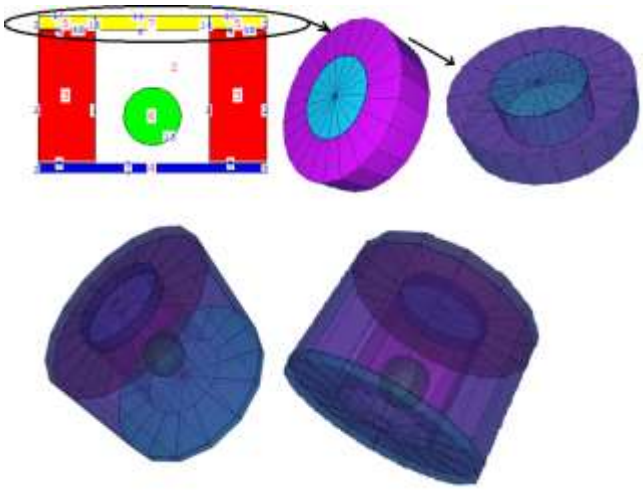

Figure 1. *Visual representation of a modeled MCNPX glass storage container for 2-D and 3-D views.*

Monte Carlo simulations use intricate geometric models to predict dose distributions, shielding effectiveness, and potential risks in various applications, such as radiation shielding for nuclear reactors and medical imaging devices. [26]. Figure 1 shows the visual representation of a modeled MCNPX glass storage container.

2.4. MCNPX Monte Carlo Simulations for Transmission

Understanding shielding effectiveness focuses mainly on determining transmission factor (TF) values for a specific substance, a crucial parameter that offers key insights into the material's absorption capabilities [28-30]. The Monte Carlo MCNPX code was utilized to model the transmission factor (TF) for the $60B_2O_3$-(25-x)GeO_2-15BaO-xWO_3 (x=0, 5, 10, 15, 20, 25) glass containers. The glass containers have been examined by initially assessing them based on the elemental properties outlined of the MCNPX code input file. The densities of these containers were specified in the input file. To measure the main and secondary gamma-ray fluxes, two identically sized detection areas were placed in front and behind the absorber material, respectively. The F4 label of the MCNPX programming language made this procedure possible. A point source located prior to the absorber glass material and the first detection zone is the origin of the isotropic behaviors. Gamma ray energy was determined for each simulation iteration using the provided source description [29-38].

3. Results and Discussions

The $60B_2O_3$-(25-x)GeO_2-15BaO-xWO_3 (x=0, 5, 10, 15, 20, 25) glass container compositions evaluated six combinations to understand their ability to block ionizing gamma rays with energy between 0.015 and 15 MeV. The gamma-ray shielding capacity of a material is strongly correlated with its density and atomic arrangement. Figure 2 shows the range of densities found in the glass containers that were evaluated.

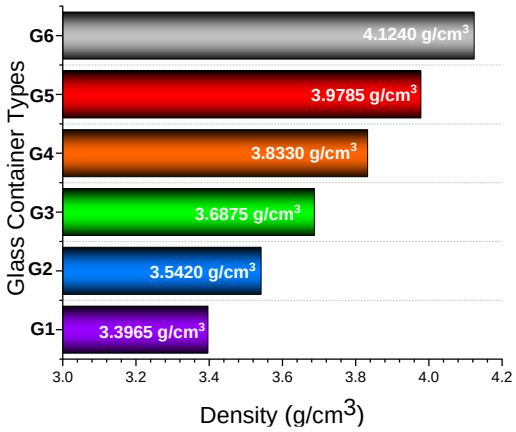

Figure 2. *Variation of investigated glass container densities.*

Figure 3 and Figure 4 display that the LAC and MAC values calculated for photon energy ranging from 0.015 to 15 MeV are higher in high density composite glass containers compared to low density composite glass container structures. Essential to gamma-ray shielding as a density-dependent factor is the linear attenuation coefficient (cm^{-1}). The linear attenuation coefficient (μ) is a constant parameter that represents the proportion of incoming photons

that are absorbed in a monoenergetic beam per unit thickness of a material.

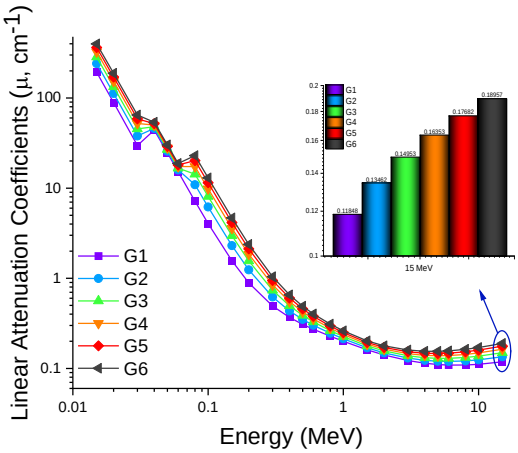

Figure 3. *Variation of linear attenuation coefficient (cm^{-1}) with photon energy (MeV) for all investigated glass containers.*

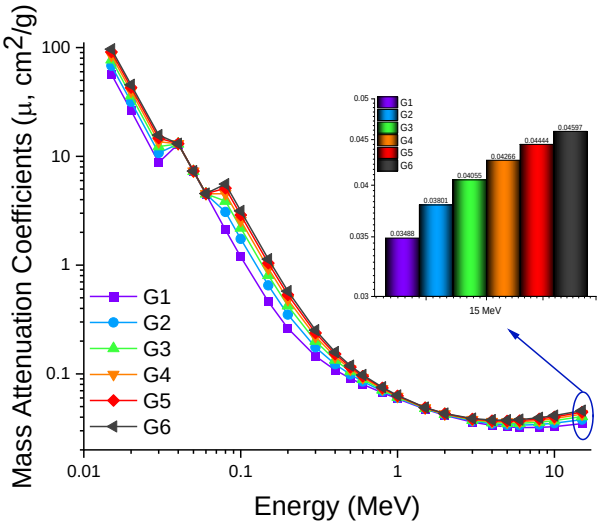

Figure 4. *Variation of mass attenuation coefficients (cm^2/g) with photon energy (MeV) for all investigated glass containers.*

As the atomic number and physical density of the absorbing substance rise, the linear attenuation coefficient increases as well. The μ values' behavior changed depending on the gamma-ray energy range. A noticeable decrease in the low energy zone has been seen as a result of the prevalence of the photoelectric effect. In the mid-energy range, the decline continued but slowed down because of the predominance of Compton scattering. Calculations of the linear attenuation coefficient showed that the G6 glass container had the greatest values across all energy levels. The graph shows how the mass attenuation coefficients (μ_m, cm^2/g) of the glass container change as the photon energies change. As the energy level rise, μm generally goes down. This trend is common because of the reduced photoelectric absorption at higher energy levels. The G6 glass container shows high μ_m values, which are associated with the large atomic numbers of lead and tungsten, indicating their prevalence in the compositions. Elements with high atomic numbers are more effective at reducing the intensity of photons through photoelectric absorption. The data acquired indicated that there were no significant numerical differences among the glass containers analyzed in the high energy range. The fundamental reason is that the differences in glass container compositions are not chemically stable, leading to an average overall difference in glass density of 0.73 g/cm3 between the G1 and G6 glass containers. For a certain energy level, the mean free path (mfp) can be found. This gives useful details about how doping and changes in chemical composition affect the interaction distance, which is especially useful for looking at differences. Figure 5 shows how the mass attenuation coefficient (mfp) changes for G1–G6 glass containers based on photon energy in megaelectronvolts (MeV). The units used are centimeters and MeV.

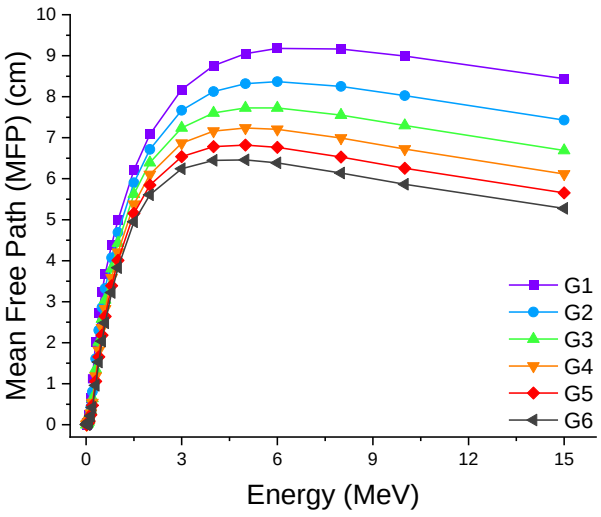

Figure 5. *Variation of mean free path (cm) with photon energy (MeV) for all investigated glass containers.*

As a function of the incoming photon energy (MeV), Figure 5 displays the mass attenuation coefficient values of the glass containers. This strongly indicates a correlation between the penetrating properties of gamma rays and the average distance they can travel. Despite the mfp value increasing with gamma-ray energy, the G6 glass container exhibited the lowest mfp values for a certain gamma-ray energy. Gamma rays of certain energy levels can closely interact with the G6 glass container, leading to more efficient absorption by the material. Examination of the mfp values of the investigated

glass groups reveals that G6 has the lowest value, as the gamma energy rises. Figure 6 and Figure 7 show the HVL and TVL values of the composite spectacles under examination. The HVL value is essential for calculating the thickness of shielding material that reduces the initial radiation intensity by half, whereas the TVL parameter decreases the radiation intensity by one-tenth. The TVL can be utilized to create a parameter similar to the HVL, that provides equivalent information. This parameter indicates the material thickness required to decrease the radiation intensity on the material by one-tenth. Tenth-value layer values exhibit higher quantitative values than half-value layer values for equivalent energy values. This condition is anticipated, and thicker shielding material is required to decrease the intensity of radiation with a specific energy value of one-tenth. The study results indicated that the G6 glass container exhibited the lowest values in one-tenth value thicknesses, despite the two parameters having distinct quantitative values for the same energy levels. The results offer additional proof that the G6 composite glass container is extremely resilient to ionizing gamma radiation. The necessary components for determining the gamma ray resistance of a material based on its attenuation characteristics are the effective atomic number (Z_{eff}) and the linearly related effective electron density (N_{eff}). Figure 8 illustrates the relationship between the value of the analyzed glass containers (Z_{eff}) and photon energy. The area had the greatest values of Zeff due to the prevalence of photoelectric contact mechanisms. A notable rise in

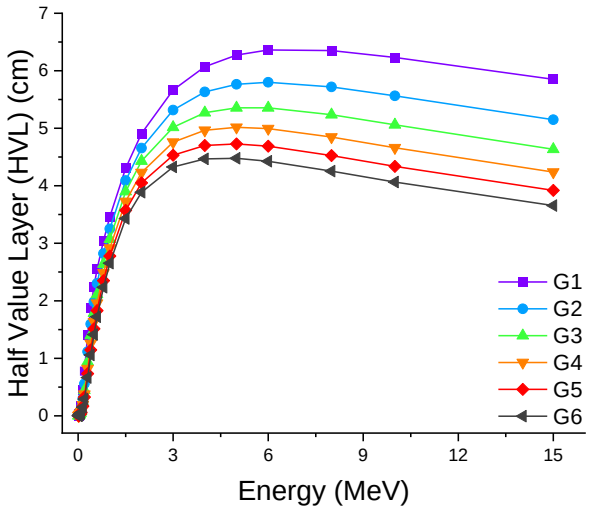

Figure 6. *Variation of the half-value layer (cm) with photon energy (MeV) for all investigated glass containers.*

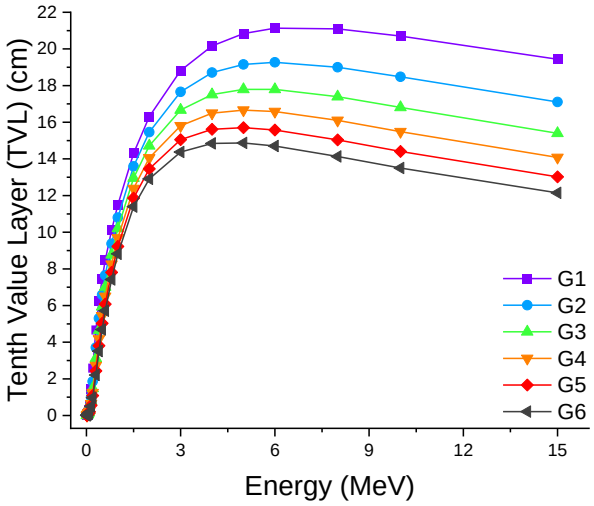

Figure 7. *Variation of the tenth-value layer (cm) with photon energy (MeV) for all investigated glass containers.*

Z_{eff} occurred in the lowest energy range due to the increase in WO_3 within the glass matrix. The Z_{eff} values in the intermediate zone decreased significantly because of the high occurrence of Compton scattering. Ultimately, in the most energy-demanding area, the emergence of Zeff was once again observed due to the majority of the occurrences linked to steam production. This ensures that the G6 with the largest m has the highest achievable Zeff. The G6 glass container exhibited the greatest Z_{eff} value based on this research. A relationship between the effective atomic number and the effective electron density (N_{eff}) is illustrated in Figure 9. The effect of scattered radiation is taken into consideration when secondary particles are present inside the medium by using the build-up factor. Consideration of the source of secondary ionizing radiation is essential. The build-up factor increases the effect of unbounded photons in order to account for dispersed photons. During the accumulating process, the multiplier takes in scattered photons that pass unintercepted. The two primary types of building factors are exposure buildup factor (EBF) and energy absorption buildup factor (EABF). The Phy-X/PSD method is used to measure the EBF and EABF terms for six glass containers with mfp values ranging from 0.5 to 40 mfp. Figure 10 illustrates the relationship between energy and exposure buildup factor (EBF) for various values of the mean free path (mfp).

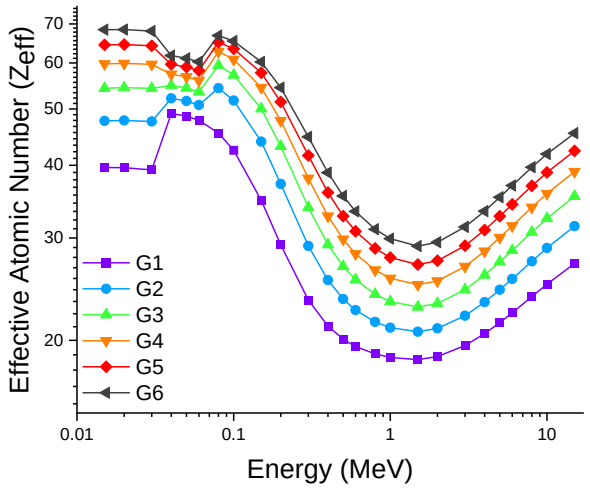

Figure 8. *Variation of effective atomic number (Z_{eff}) with photon energy (MeV) for all investigated glass containers.*

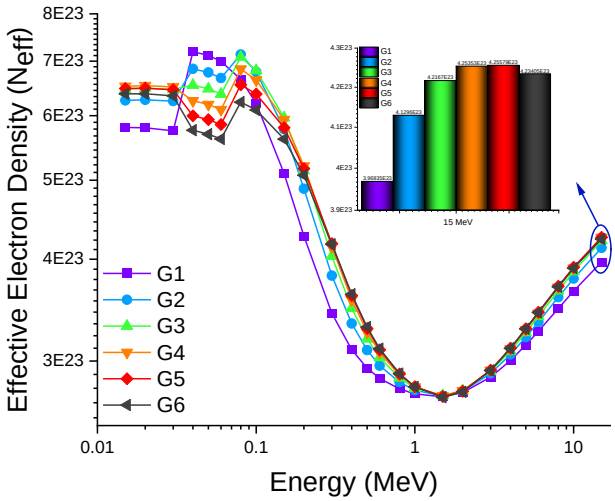

Figure 9. *Variation of effective electron density (N_{eff}, electrons/g) with photon energy (MeV) for all investigated glass containers.*

Various types of chemical reactions occur in various places in nature. The binding energies of elements with high atomic numbers are closely aligned with their atomic numbers, causing the first area to peak. The EBF values remain steady inside the Compton resonance zone. Pair production is the third priority area due to absorption processes leading to a little rise in EBF. The G6 glass container has the lowest EBF value that was discovered. This proves that materials are effective at reducing the effects of gamma radiation. The best isolated glass container was G6, as it had the lowest EBF values out of all the specimens tested. Figure 11 shows a consistent pattern when graphing the energy absorption buildup factor (EABF) against photon energy (MeV) ranging from 5 to 40 mfp. In the last phase, the MCNPX algorithm was used to obtain the TF values for all of the glass containers. To achieve this objective, a transmission structure was devised, as seen in Figure 12.

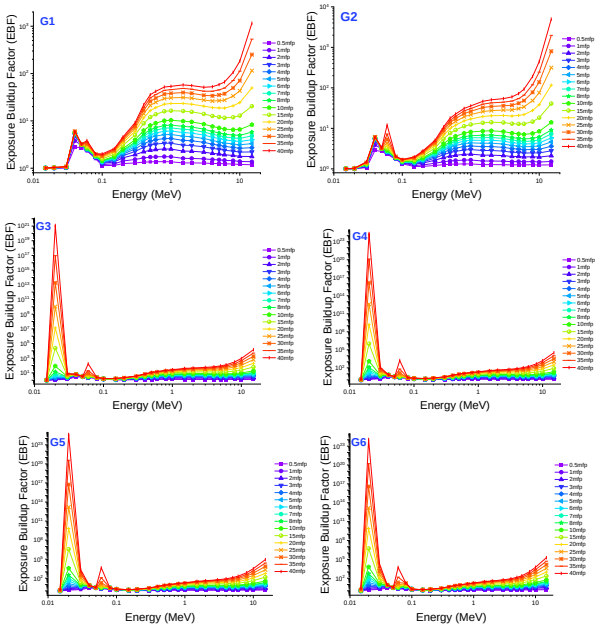

Figure 10. *Variation of exposure buildup factors (EBF) of all investigated glass containers at different mean free path values.*

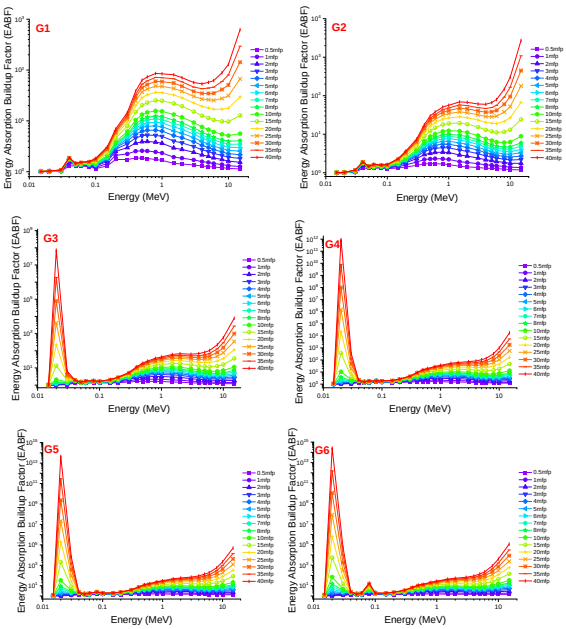

Figure 11. *Variation of energy absoption buildup factors (EABF) of all investigated glass containers at different mean free path values.*

The current study used the F4 tally mesh, a tool that calculates the average flux of photons inside a certain point or cell. Two separate F4 tally meshes were generated, one placed in front of the glass container and the other positioned behind it. TF

values were calculated for each glass container by adjusting the energy values and thicknesses. This method was used to study how the thickness and energy affected the TF behaviors of the glass containers being studied. The graph shows a negative association between TF values and glass container thickness, suggesting a decreasing trend as TF values grow. The impact of the glass attenuator remains consistent across all energy levels, as it exhibits a higher absorption capacity for gamma rays at specified depths

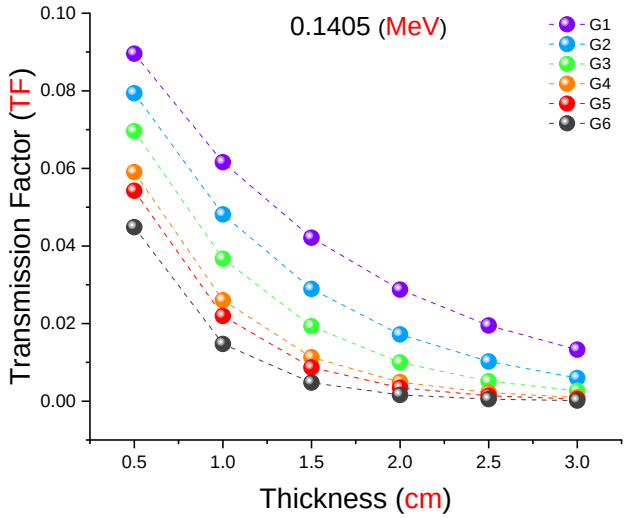

Figure 12. *Transmission Factors (TFs) of all investigated glass containers as a function of used radioisotope energy (MeV) at different glass thicknesses.*

In particular, the G6 glass container exhibits much higher TF values compared to the other containers. This correlates closely with the anticipated gamma-ray absorption properties and the TF estimates obtained from simulations. This highlights the potential of the G6 glass container as a more advantageous option for applications involving gamma-ray shielding.

4. Conclusions

This research resulted in composite glass containers with the composition $60B_2O_3$-(25-x)GeO_2-15BaO-xWO_3 (where x = 0, 5, 10, 15, 20, 25). The development of these containers was a direct outcome of the research findings. These studies indicate that augmenting the density of WO_3 in glass results in an improvement in the material's radiation resistance. The presence of WO_3 results in the introduction of radiation into the system. The presence of WO_3 has a noticeable impact on the attenuation properties of radiation, as observed at the surface. The fact that the G6 glass container with the most WO_3 has higher photon attenuation means that the WO_3 reinforcement stops nuclear radiation from getting into the container. Based on the scientific community's research on the use of lead-free WO_3 in composite glass containers, it is suggested that a future study might be conducted using this material. The essential importance lies in providing secure and efficient transportation of Tc-99m within medical and industrial contexts. In order to accomplish this objective, the utilization of specifically designed glass containers plays a crucial role in the regulation of gamma rays during the transportation of Tc-99m. Hence, the primary focus is on the advancement and application of these receptacles to protect individuals and the environment against the detrimental effects of radiation exposure. Getting gamma rays to be absorbed by packaging efficiently is very important for transporting Tc-99m safely and effectively. This has a big impact on the fields of nuclear medicine and healthcare.

Author Statements:

- **Ethical approval:** The conducted research is not related to either human or animal use.
- **Conflict of interest:** The author declare that they have no known competing financial interests or personal relationships that could have appeared to influence the work reported in this paper
- **Acknowledgement:** The author declare that they have nobody or no-company to acknowledge.
- **Funding information:** The author declare that there is no funding to be acknowledged.
- **Data availability statement:** The data that support the findings of this study are available on request from the corresponding author. The data are not publicly available due to privacy or ethical restrictions.

References

[1] Singh J, Singh H, Sharma J, Singh T, Singh PS. (2018). Fusible alloys: a potential candidate for gamma rays shield design. *Prog. Nucl. Energy*, 106,387-395 https://doi.org/10.1016/j.pnucene.2018.04.002.

[2] Erdemir, Rabiye Uslu, Kilic, Gokhan, Sen Baykal, Duygu, ALMisned, Ghada, Issa, Shams A. M., Zakaly, Hesham M. H., Ene, Antoaneta and Tekin, Huseyin Ozan. (2022). Diagnostic and therapeutic radioisotopes in nuclear medicine: Determination of gamma-ray transmission factors and safety competencies of high-dense and transparent glassy shields. *Open Chemistry*, 20,517-524. https://doi.org/10.1515/chem-2022-0167.

[3]Dudley T. Goodhead, (2009). Understanding and characterisation of the risks to human health from exposure to low levels of radiation, *Radiation*

Protection Dosimetry, 137(1-2);109–117, https://doi.org/10.1093/rpd/ncp191.

[4] Mazzi, U., Schibli, R., Pietzsch, H.J., Künstler, J.U., Spies, H. (2007). Technetium in Medicine. In: Zolle, I. (eds) Technetium-99m Pharmaceuticals. Springer, Berlin, Heidelberg. https://doi.org/10.1007/978-3-540-33990-8_2.

[5] William C. Eckelman, (2009). Unparalleled Contribution of Technetium-99m to Medicine Over 5 Decades, *JACC: Cardiovascular Imaging*, 2(3); 364-368, https://doi.org/10.1016/j.jcmg.2008.12.013.

[6]N. Singh, K.J. Singh, K. Singh, H. Singh (2004). Comparative study of lead borate and bismuth lead borate glass systems as gamma-radiation shielding materials *Nucl. Instrum. Methods Phys. Res. B*, 225;305-309, https://doi.org/10.1016/j.nimb.2004.05.016.

[7] Duygu Sen Baykal, G. Kilic, Erkan Ilik, E. Kavaz, Ghada ALMisned, R.B. Cakirli, H.O. Tekin, (2023). Designing a Lead-free and high-density glass for radiation facilities: Synthesis, physical, optical, structural, and experimental gamma-ray transmission properties of newly designed barium-borosilicate glass sample, *Journal of Alloys and Compounds*, 965,171392, https://doi.org/10.1016/j.jallcom.2023.171392.

[8]Ab.Latif Wani, Anjum Ara, Jawed Ahmad Usmani (2015). Lead toxicity: a review Interdisc. Toxicol. https://doi.org/10.1515/intox-2015-0009.

[9]Monisha Jaıshankar, Tenzin Tseten, Naresh Anbalagan, BlessyB. Mathew, KrishnamurthyN. Beeregowda Toxicity, mechanism and health effects of some heavy metals Inter.Toxicol. 7(2), https://doi.org/10.2478/intox-2014-0009.

[10] Muhammad Shahid, Sana Khalid, Ghulam Abbas, Naeem Shahid, Muhammad Nadeem, Muhammad Sabir, Muhammad Aslam & Camille Dumat (2015). Heavy metal stress and crop productivity K. Hakeem (Ed.), Crop Production and Global EnvironmentalIssues, Springer, Cham, https://doi.org/10.1007/978-3-319-23162-4_1.

[11]Muhammad Shahid, Camille Dumat, Bertrand Pourrut, Muhammad Sabir, Eric Pinelli (2014). Assessing the effect of metal speciation on lead toxicity to Vicia faba pigment contents,*J.Geochem.Explor*. https://doi.org/10.1016/j.gexplo.2014.01.003.

[12] D. A. Gidlow, (2004). In-depth review, Lead Toxicity, *Occupational Medicine* 54:76–81 https://doi.org/10.1093/occmed/kqh0192003.

[13] Nadin Jamal Abu Al Roos, Noorfatin AidaBaharul Amin, Rafidah Zainon. (2019). Conventional and New Lead-free Radiation Shielding Materials for Radiation Protection in Nuclear Medicine: a review, *Radiation Physics and Chemistry* 165; 108439 https://doi.org/10.1016/j.radphyschem.2019.108439

[14]Laal Marjan. (2013). Innovation process in medical imaging, *Procedia-Social and Behavioural Sciences*,81;60-64 https://doi.org/10.1016/j.sbspro.2013.06.388.

[15] Smith-Bindman R., Lipson J., Marcus R., et al. (2009). Radiation dose associated with common computed tomography examinations and the associated lifetime attributable risk of cancer, *Archives of internal medicine*, 169(22);2078–2086. https://doi.org/10.1001/archinternmed.2009.427.

[16] E. Browne, J.K. Tuli (2011). Nuclear data sheets for A=99 Nucl.Data Sheets, https://doi.org/10.1016/j.nds.2011.01.001.

[17] AlMisned G, Sen Baykal D, Ilik E, Abuzaid M, Issa SAM, Kilic G, Zakaly HMH, Ene A, Tekin HO. (2023). Tungsten (VI) oxide reinforced antimony glasses for radiation safety applications: A throughout investigation for determination of radiation shielding properties and transmission factors. *Heliyon.* 30;9(7):e17838. https://doi.org/10.1016/j.heliyon.2023.e17838.

[18] Abouhaswa A.S., Zakaly H.M.H., Issa S.A.M., Rashad M., Pyshkina M., Tekin H.O., ElMallawany R., Mostafa M.Y.A. (2021). Synthesis, physical, optical, mechanical, and radiation attenuation properties of TiO_2–Na_2O–Bi_2O_3–B_2O_3 glasses. *Ceram.Int.*, 47(1);185-204 https://doi.org/10.1016/j.ceramint.2020.08.122.

[19] M.S. Al-Buriahi, C. Sriwunkum, H. Arslan, et al. (2020). Investigation of barium borate glasses for radiation shielding applications *Appl. Phys. A*, 126, 68, https://doi.org/10.1007/s00339-019-3254-9.

[20] U. Kara, E. Kavaz, ShamsA.M.Issa, M. Rashad, G. Susoy, A.M.A. Mostafa, N. Yildiz Yorgun, H.O. Tekin. (2020). Optical, structural and nuclear radiation shielding properties of Li2B4O7 glasses: efect of boron mineral additive. *Applied Physics A*, 126; 261, https://doi.org/10.1007/s00339-020-3397-8.

[21] H.O. Tekin, V.P. Singh, T. Manici. (2017). Effects of micro-sized and nano-sized WO3 on mass attenauation coefficients of concrete by using MCNPX code *Appl. Radiat. Isot.*, 121;122-125. https://doi.org/10.1016/j.apradiso.2016.12.040.

[22] M.M. Hosamani, N.M. Badiger (2018). Determination of effective atomic number of composite materials using backscattered gamma photons a novel method *Chem Phys. Lett*, 695;94-98. https://doi.org/10.1016/j.cplett.2018.02.012.

[23] Erdem Şakar, Özgür Fırat Özpolat, Bünyamin Alım, M.I. Sayyed, Murat Kurudirek, (2020). Phy-X / PSD: Development of a user friendly online software for calculation of parameters relevant to radiation shielding and dosimetry, *Radiation Physics and Chemistry*, 166;108496, , https://doi.org/10.1016/j.radphyschem.2019.108496

[24]H.O. Tekin, Ghada ALMisned, ShamsA.M. Issa, Hesham M.H. Zakaly (2022). A rapid and direct method for half value layer calculations for nuclear safety studies using MCNPX Monte Carlo code *Nucl. Eng.,Technol*., 54(9);3317-3323, https://doi.org/10.1016/j.net.2022.03.037.

[25] Ghada ALMisned, Kadir Günoğlu, Hatice Varol Özkavak, Duygu Sen Baykal, H.O. Tekin, Nurdan Karpuz, Iskender Akkurt, (2023). An investigation on gamma-ray and neutron attenuation properties of multi layered Al/B4C composite, *Materials Today*

Communications, 36;106813 , https://doi.org/10.1016/j.mtcomm.2023.106813.

[26] J. Briesmeister, MCNP—a General Monte Carlo Code for Neutron and Photon Transport, National Laboratory, Los Alamos, 2000 Report LA13709-M, version 4C.

[27] Hançerlıoğlu, a. (2006). Monte carlo sımulatıon method and mcnp code system. *Kastamonu education journal*, 14(2), 545-556.

[28] R. Boodaghi Malidarre, I. Akkurt (2021). Monte Carlo simulation study on TeO_2–Bi_2O–PbO–MgO–B_2O_3 glass for neutron-gamma ^{252}Cf source *J. Mater. Sci: Mater. Electron*, 32;11666–11682 https://doi.org/10.1007/s10854-021-05776-y.

[29] Ghada ALMisned, Hesham M.H. Zakaly, Fatema T. Ali, Shams A.M. Issa, Antoaneta Ene, Gokhan Kilic, V. Ivanov, H.O. Tekin, (2022). A closer look at the efficiency calibration of LaBr3(Ce) and NaI(Tl) scintillation detectors using MCNPX for various types of nuclear investigations, *Heliyon*, 8(10);e10839 https://doi.org/10.1016/j.heliyon.2022.e10839.

[30] W. Marltan, P. Venkateswara Rao, H.O. Tekin, M.I. Sayyed, R. Klement, D. Galusek, G. Lakshminarayana, P. Syam Prasad, N. Veeraiah, (2019). Analysis of red mud doped Bi2O3-B2O3-BaO glasses for application as glass solder in radiation shield repair using MCNPX simulation, *Ceramics International*, 45(6);7619-7626 https://doi.org/10.1016/j.ceramint.2019.01.058.

[31] Ghada ALMisned, Wiam Elshami, Gokhan Kilic, Erkan Ilik, Elaf Rabaa, Hesham M. H. Zakaly, Antoaneta Ene, Huseyin O. Tekin. (2023). Exploring the Radioprotective Indium (III) Oxide Screens for Mammography Scans Using a Three-Layer Heterogeneous Breast Phantom and MCNPX: A Comparative Study Using Clinical Findings. *Medicina* 59;327. https://doi.org/10.3390/medicina59020327.

[32] RSICC Computer Code Collection, MCNPX User's Manual Version 2.4.0, in: MonteCarlo N-Particle Transport Code System for Multiple and High Energy Applications, 2002.

[33] Mohammad W. Marashdeh, Ibrahim F. Al-Hamarneh, Eid M. Abdel Munem, , A. A. Tajuddin, A. Ariffin, Saleh Al-Omari. (2015). Determining the mass attenuation coefficient, effective atomic number, and electron density of raw wood and binderless particleboards of Rhizophora spp. by using Monte Carlo simulation, *Results in Physics*, 5;228-234. https://doi.org/10.1016/j.rinp.2015.08.009.

[34] E. Kavaz, N. Ekinci, H.O. Tekin, M.I. Sayyed, B. Aygün, U. Perişanoğlu, (2019). Estimation of gamma radiation shielding qualification of newly developed glasses by using WinXCOM and MCNPX code, *Progress in Nuclear Energy*, 115;12-20 https://doi.org/10.1016/j.pnucene.2019.03.029.

[35] EMİKÖNEL, S., & AKKURT, I. (2023). Transmission Rate of Fabric to Test Radiation Shielding Properties. International Journal of Computational and Experimental Science and Engineering, 9(4), 409–411. DOI:10.22399/ijcesen.1376597

[36] COŞKUN, A., ÇETİN, B., YİĞİTOĞLU, İbrahim, & CANIMKURBEY, B. (2023). Theoretical and Experimental Investigation of Gamma Shielding Properties of TiO2 and PbO Coated Glasses. International Journal of Computational and Experimental Science and Engineering, 9(4), 398–401. DOI:10.22399/ijcesen.1367747

[37] Şahmaran, T., & TUĞRUL, T. (2023). Investigation of Shielding Parameters of Fast Neutrons for Some Chemotherapy Drugs by Different Calculation Methods . International Journal of Computational and Experimental Science and Engineering, 9(4), 388–393. DOI:10.22399/ijcesen.1366006

[38] SAVAŞ, Y., BAŞARAN, B., & ÇETİN, B. (2023). The Effect of Marble Powder Additive at Different Ratios on the Radiation Absorption Parameters of Barite Based Concretes. International Journal of Computational and Experimental Science and Engineering, 9(4), 376–381. DOI:10.22399/ijcesen.1322248